Published in final edited form as:
Cancer Res. 2010 October 1; 70(19): 7455–7464. doi:10.1158/0008-5472.CAN-10-0736.

Targeting Stat3 in the myeloid compartment drastically improves the in vivo antitumor functions of adoptively transferred T cells

Andreas Herrmann[1], **Marcin Kortylewski**[1], **Maciej Kujawski**[1], **Chunyan Zhang**[1], **Karen Reckamp**[2], **Brian Armstrong**[3], **Lin Wang**[1,4], **Claudia Kowolik**[5], **Jiehui Deng**[1,4], **Figlin Robert**[2], and **Hua Yu**[1]

[1]Department of Cancer Immunotherapeutics and Tumor Immunology, 1500 East Duarte Road Duarte, CA 91010-3000, USA

[2]Medical Oncology, 1500 East Duarte Road Duarte, CA 91010-3000, USA

[3]Department of Neurosciences, 1500 East Duarte Road Duarte, CA 91010-3000, USA

[4]Graduate School of Biological Science, 1500 East Duarte Road Duarte, CA 91010-3000, USA

[5]Molecular Medicine, Beckman Research Institute at the City of Hope National Medical Center, 1500 East Duarte Road Duarte, CA 91010-3000, USA

Abstract

Improving effector T cell functions is highly desirable for preventive or therapeutic interventions of diverse diseases. Stat3 in the myeloid compartment constrains Th-1 type immunity, dampening natural and induced antitumor immune responses. We have recently developed an *in vivo* siRNA delivery platform by conjugating a TLR9 agonist with siRNA that efficiently targets myeloid and B cells. Here we show that either ablating the *Stat3* alleles in the myeloid compartment and B cells combined with CpG triggering or administrating the CpG-*Stat3*siRNA conjugates drastically augments effector functions of adoptively transferred $CD8^+$ T cells. Specifically, we demonstrate that both approaches are capable of increasing dendritic cell and $CD8^+$ T cell engagement in tumor draining lymph nodes. Furthermore, both approaches can significantly activate the transferred $CD8^+$ T cells *in vivo*, upregulating effector molecules such as perforin, granzyme B and IFN-γ. Intravital multiphoton microscopy reveals that *Stat3* silencing combined with CpG triggering greatly increases killing activity and tumor infiltration of transferred T cells. These results suggest the use of CpG-*Stat3*siRNA, and possibly other Stat3 inhibitors, as a potent adjuvant to improve T cell therapies.

Introduction

Immunotherapies have shown promise for the prevention and treatment of various diseases (1–3). For effective vaccination against viral and other pathogen infections and for clinical benefits of cancer immunotherapies, optimizing *in vivo* functions of $CD8^+$ T effector cells is critical (4–7). However, T cell effector functions are often weakened in individuals with chronic infections and/or malignancies (8–10). Although adoptive T cell therapy has shown promise for treating viral infection and cancer (11), the requirement of extensive *ex vivo*

Correspondence should be addressed to Marcin Kortylewski: mkortylewski@coh.org or Hua Yu: hyu@coh.org, Department of Cancer Immunotherapeutics and Tumor Immunology, Beckman Research Institute, City of Hope National Medical Center, 1500 E. Duarte Road, Duarte, CA 91010-3000.

Disclosure of Potential Conflicts of Interest
No potential conflicts of interest were disclosed.

manipulation to expand, activate and to potentially increase homing of effector functions of T cells to tumor sites in the hosts limits its application (8,9). Even when the T cells have been optimally engineered and activated *ex vivo*, their activity against tumor cells often fails to persist (12,13). This is in part caused by the hostile tumor immunologic environment that dampens the efficacies of T cells activated *ex vivo* (5,14,15). It is therefore highly desirable to be able to efficiently upregulate effector functions of $CD8^+$ T cells *in vivo*, not only to reduce the requirement of extensive *ex vivo* manipulation of T cells but also to circumvent the immunosuppression associated with chronic infections and/or cancer.

We and others have recently identified Stat3 as negative regulator of Th1 immunity (16–19). In the setting of malignancy, Stat3 is persistently activated not only in tumor cells but also in tumor-associated myeloid cells as well as regulatory T cells (16,20). Inhibiting Stat3 in either tumor cells or tumor myeloid cells can elicit Th1 antitumor innate and adaptive immune responses, which is accompanied by an increase in tumor infiltrating $CD8^+$ T cells and decrease in tumor regulatory T cells (17). However, for potential clinical translation of these findings, it is critical to determine whether targeting Stat3 in myeloid cells can alter the effector functions of adoptively transferred $CD8^+$ T cells.

It has also been shown that certain toll-like receptor signaling activates Stat3, which in turn constrains the magnitude of innate immune responses (21–23). Ablating *Stat3* in the myeloid compartment and B cells drastically improves the efficacy of TLR9 agonist CpG-induced antitumor immune responses (24). By conjugating CpG with siRNA, we have recently developed a novel *in vivo* siRNA delivery technology platform achieving targeted delivery and gene silencing in myeloid cells and B cells, as well as immune activation (25). In the current study, we explore the feasibility of utilizing CpG-*Stat3*siRNA to improve the effector functions of adoptively transferred $CD8^+$ T cells *in vivo*, thereby developing an approach to alleviate the extensive *ex vivo* manipulations while improving the antitumor efficacies of transferred T cells.

Materials and Methods

Cells

Murine B16-F10 melanoma cells and B16 cells expressing ovalbumin ($B16^{OVA}$) were generously provided by Drs. D. M. Pardoll (J. Hopkins, Baltimore, MD) and J. Mule (Moffitt Cancer Center, Tampa, FL), respectively. The B16 cells expressed melanoma-specific HMB-45 antigen as assessed using intracellular staining and flow cytometry (data not shown). The expression of exogenous OVA antigen and B16 cell-specific endogenous TRP2 and p15E antigens was confirmed by ELISPOT assays performed within the last six months. The ability of these cells to form melanoma in C57BL/6 mice and to elicit OVA-specific response was monitored.

Mice

Stat3^{flox} mice were kindly provided by S. Akira (Osaka University, Osaka, Japan). Ova TCR (OT-I), Rag1(ko)Momj/B6.129S7, and Mx1-Cre transgenic mice were purchased from the Jackson Laboratory. *Stat3*^{flox} and *Mx1-Cre* mice were crossed and treated with poly(I:C) to obtain *Stat3* conditional knockout in the hematopoietic system as described previously (26). C57BL/6 mice were purchased from the National Cancer Institute (Frederick, MD). CD11c(YFP)-Tg(BDC2.5)NOD mice were kindly provided by Dr. Chih-Pin Liu (City of Hope, Duarte, CA). Mouse care and experimental procedures were performed under pathogen-free conditions in accordance with established institutional guidance and approved protocols from the Research Animal Care Committees of the City of Hope.

In vivo experiments and T cell adoptive transfer

B16 or B16^{OVA} cells (10^6 or 2.5×10^5) were injected *s.c.* into *Rag1*$^{-/-}$ mice, C57BL/6 wild type or *Stat3*^{flox} mice, respectively. 8–10 × 10^6 CD8 or CD8$^{OT\text{-}I}$ T cells were adoptively transferred when tumors reached an average diameter of 5 mm via retro-orbital route. T cells were isolated from spleens and lymph nodes of donor mice using negative selection (EasySep, StemCell Technologies) or MACS cell separation system positive selection (Miltenyi Biotec). Fluorescent cell labeling was performed using CFSE or CMAC CellTracker (Invitrogen), according to the manufacturer instructions.

TLR9 agonist treatment

B16^{OVA} tumor bearing *Stat3*^{flox} mice received 5 μg (0.78 nmole) phosphothioated CpG-ODN 1668 (TCCATGACGTTCCTGATGCT) injected peritumorally 5 h prior to CD8$^{OT\text{-}I}$ T cell adoptive transfer. C57BL/6 wild-type bearing B16^{OVA} tumors were treated every other day with 19.2 μg (0.78 nmole) CpG-*luciferase*-siRNA, CpG-scrambled-RNA, or CpG-*Stat3*siRNA. Adoptive T cell transfer was performed 24 h after the first CpG-siRNA treatment.

Flow Cytometry

Cell suspensions were prepared from lymph nodes and tumor tissues as described previously, followed by staining with different combinations of fluorophore conjugated antibodies against CD8, CD69, CD4, CD25, FoxP3, IFN-γ, and granzyme B (BD Biosciences). Flow data were acquired using FACScalibur (BD Biosciences) and analyzed by FlowJo software (Tree Star).

Indirect Immunofluorescence

Tissue sections were fixed with 2% paraformaldehyde, permeabilized in methanol, and blocked in PBS containing 10% goat serum (Sigma) and 2.5% mouse serum (Sigma). Sections were incubated overnight with primary antibodies (αDendritic Cell Marker, clone 33D1, eBioscience; Perforin1, Santa Cruz) diluted 1:50 in PBS (supplemented with goat and mouse sera) and for 1 h with fluorophore-conjugated secondary antibodies (Invitrogen) after washing thrice with PBS. Immunofluorescent stainings were analyzed by confocal microscopy (LSM510Meta, Zeiss).

Intravital multiphoton microscopy (IVMPM)

Tumor bearing mice were anesthetized with an isoflurane/oxygen mixture. Fifteen minutes prior to imaging procedure, mice were given 100 μg dextran-rhodamine (Invitrogen) and 10 μg Annexin V FITC (BioVision) *i.v.*. Extracellular matrix (ECM) emission signals were given by second harmonic generation at λ[excit] = 890 nm (Coherent Chameleon Ultra II Ti:Sa laser). For recording fluoresceine and rhodamine emission, λ[excit] = 860 nm was used, coumarin emission signals were recorded at λ[excit] = 730 nm. Labeling of CD8$^{OT\text{-}I}$ cells with CMAC or CFSE cell tracker (Invitrogen) was performed according to manufacturer instructions. Images were acquired using an Ultima Multiphoton Microscopy System (Prairie Technologies) equipped with Prairie View software and non-descanned Hamamatsu PhotoMultiplier Tubes. Images were collected in a 512×512, 16-bit, TIFF format. Composite images were created using Image Pro Plus professional imaging software (Media Cybernetics, Bethesda, MD).

Enzyme-linked immunosorbent spot (ELISPOT) assay

5×10^5 cells isolated from tumor draining lymph nodes of tumor bearing mice as well as from lymph nodes of naïve mice were seeded into a 96-well filtration plate in the absence or presence of 10 μg/ml peptide (TRP-2^{SVYDFFVWL}, OVA^{SIINFEKL}, AnaSpec, CA;

p15E^{KSPWFTTL} generated by the DNA/RNA and Protein Synthesis Core Facility at the City of Hope) for 24 h at 37°C. Peptide-specific Granzyme B and IFN-γ positive spots were detected according to the manufacturer's instructions (R&D Systems, Diaclone), and manually counted using a binocular microscope.

In vivo CTL killing assay

Splenocytes of syngeneic animals were harvested and split into two populations. Target cell population was pulsed with 2 μg/ml OVA^{SIINFEKL} peptide for 2 h at 37°C followed by CFSE^{HI} (10 μM) fluorescent labeling while the control cell population remained unpulsed but was labeled CFSE^{LO} (1 μM). Equal numbers of CFSE^{HI} and CFSE^{LO} cells were mixed and adoptively transferred *i.v.* into tumor bearing animals. Each animal received 20 × 10^6 cells. CTL cytotoxic effects were analyzed by flow cytometry (FACScalibur, BD).

Results

Ablating *Stat3* in myeloid cells improves effector functions of transferred CD8$^+$ T cells

Since T cell engagement by antigen presenting cells is a critical step for T cell priming (27–29), we monitored cell to cell contacts of adoptively transferred CD8^{OT-I} T cells and dendritic cells (DCs) in B16^{OVA} tumor bearing mice, which received CpG-ODN 5 h prior to T cell transfer. Intravital multiphoton microscopy imaging of the tumor draining lymph node was carried out 15–18 h after adoptive transfer. Results from the imaging revealed significantly increased engagement of CD8^{OT-I} T cells by CpG$^+$ myeloid cells in mice with *Stat3*$^{-/-}$ hematopoietic cells (Fig. 1*A*, *top*, *C*). Immunofluorescent staining of frozen sections prepared from tumor draining lymph nodes confirmed CpG-ODN internalization by DCs (Fig. 1*A*, *bottom*). Results from flow cytometric analysis showed that adoptively transferred CD8^{OT-I} T cells underwent rapid activation upon *Stat3* ablation in the myeloid compartment, as indicated by higher CD69 expression by the T cells, relative to those from *Stat3*$^{+/+}$ mice (Fig. 1*C*). Clonal expansion of adoptively transferred CD8^{OT-I} T cells represents the final step of T cell priming. We therefore tested the *in vivo* effect of *Stat3* ablation in the myeloid compartment on transferred T cell clonal expansion. CD8^{OT-I} T cells were loaded with CFSE cell tracker and transferred into B16^{OVA} tumor bearing mice. T cell expansion was assessed 16 h after adoptive transfer. Flow cytometric analysis showed proliferation of CD8^{OT-I} T cells in the tumor draining lymph node of mice with *Stat3*$^{-/-}$ but not *Stat3*$^{+/+}$ myeloid compartment. Notably, proliferation of the transferred T cells was not detectable in the contra-lateral lymph node of *Stat3*$^{-/-}$ mice, indicating peritumoral CpG-ODN administration results in tumor-associated CD8$^+$ T cell expansion (Fig. 1*D*).

Stat3 ablation improves cytolytic activity and tumor infiltration of transferred CD8^{OT-I} cells

Both homing capacity and cytolytic activity of transferred CD8$^+$ T cells are limited in tumor-bearing hosts. We therefore assessed the impact of *Stat3* ablation in the myeloid compartment on CTL effector functions upon CpG triggering. Immunofluorescent staining of microsections of tumor draining lymph nodes prepared from mice challenged with B16^{OVA} tumor cells showed that perforin 1 expression was considerably increased in transferred CD8^{OT-I} T cells in recipient mice with *Stat3*$^{-/-}$ myeloid compartments (Fig. 2*A*). Notably, perforin expression was not restricted to CD8^{OT-I} T cells but was also observed in host lymphocytes, suggesting that perforin upregulation occurs in host CD8$^+$ T cells and NK cells upon genetic *Stat3* deletion in myeloid cells and CpG administration. In addition, granzyme B and IFN-γ expression by adoptively transferred antigen-specific CD8^{OT-I} T cells was markedly increased upon *Stat3* ablation in myeloid cells (Fig. 2*B*). *In vivo* CTL killing assay further indicated that the elevated expression of granzyme B and IFN-γ led to an effector CTL population phenotype with strong and rapid cytolytic activity against tumor antigen peptide-pulsed, CFSE-labeled syngeneic splenocytes (Fig. 2*C*). However, the

CFSE^{HI} target cell population that resisted CTL killing in *Stat3*$^{+/+}$ mice at an earlier time point (6 h) became more susceptible at a later point (15 h). But unlike efficient CTL killing activity in mice with *Stat3*$^{-/-}$ myeloid cells, CFSE^{HI} target cells remained resistant to CTL killing in *Stat3*$^{+/+}$ mice after 20 h. Although adoptively transferred CD8$^{OT\text{-}I}$ T cells are functionally active in *Stat3*$^{+/+}$ mice, their adaptive tolerance indicates partial T cell anergy (30). Thus, Stat3 hinders effector CTL maturation induced by combining T cell therapy with TLR9 agonist administration.

We next examined tumor infiltration of CMAC labeled and adoptively transferred CD8$^{OT\text{-}I}$ T cells. Results from flow cytometric analysis show improved effector CTL^{CMAC+} tumor infiltration in *Stat3*$^{-/-}$ tumor bearing mice 24 h after adoptive transfer (Fig. 2*D*), correlating with enhanced VCAM-1 expression in tumor tissue (Supplementary Fig. 1). VCAM-1 expression is thought to facilitate CD8^{+} T cell trafficking to the tumor (31–33). Taken together, our data so far indicate that silencing *Stat3* in the myeloid compartment can improve effector CTL maturation/killing activity and tumor infiltration of transferred CD8^{+} T cells.

Enhancing effector functions of transferred CD8^{+} T cells by CpG-*Stat3*siRNA conjugate

Since ablating *Stat3* in the hematopoietic system in conjunction with CpG administration improves drastically effector functions of transferred CD8^{+} T cells, we tested CpG-*Stat3*siRNA as a therapeutic molecule in this setting. We monitored the cellular uptake of red fluorescently labeled CpG-*Stat3*siRNA in naïve transgenic mice with a yellow fluorescent dendritic cell population, due to expression of YFP under control of the CD11c promoter. Fluorescent CpG-*Stat3*siRNA or fluorescent CpG without the siRNA moiety were injected *s.c.*, followed by intravital multiphoton microscopy analysis of the inguinal lymph nodes 2 h after injection. Both CpG as well as CpG-*Stat3*siRNA were efficiently uptaken by CD11c(YFP)$^{+}$ cells (Fig. 3*A*, *top*), indicating that the siRNA moiety does not affect cellular internalization.

Early activation of adoptively transferred CD8$^{OT\text{-}I}$ T cells upon treatment with either CpG-*Stat3*siRNA or control CpG-*luciferase*-siRNA was assessed in tumor draining lymph nodes of B16^{OVA} tumor-bearing mice. CpG-*luciferase*-siRNA treated mice, CD8$^{OT\text{-}I}$ T cell recipient mice, and untreated mice were included as controls. Combined treatment with CpG-*Stat3*siRNA and CD8$^{OT\text{-}I}$ T cell adoptive transfer resulted in augmented CD8^{+} T cell activation compared to treatment with CpG-*luciferase*-siRNA and T cell transfer, CpG-*luciferase*-siRNA alone, or transferred CD8$^{OT\text{-}I}$ T cells alone, or untreated control as shown by CD69 surface expression analysis (Fig. 3*A*, *bottom*). Moreover, Stat3 knockdown in CD11c^{+} cells achieved by repeated CpG-*Stat3*siRNA administration (Fig. 3*B*) significantly increased granzyme B and IFN-γ expression by adoptively transferred CD8$^{OT\text{-}I}$ T cells (Fig. 3*C*). Notably, CpG-*luciferase*-siRNA treatment failed to induce maturation of adoptively transferred CD8$^{OT\text{-}I}$ T cells into a CTL phenotype, since granzyme B and IFN-γ production is not significantly changed compared to adoptively transferred CD8$^{OT\text{-}I}$ T cells alone. These observations suggest that targeting *Stat3* in myeloid cells by CpG-siRNA improves key effector functions of transferred CD8^{+} T cells. Finally, we examined tumor infiltration of fluorescently labeled and transferred CD8$^{OT\text{-}I}$ T cells. While CpG-*luciferase*-siRNA treatment did not improve tumor infiltration of transferred CD8$^{OT\text{-}I}$ T cells, CpG-*Stat3*siRNA administration increased T cell tumor infiltration (Fig. 3*D*).

The impact of improved effector functions of transferred CD8^{+} T cells by CpG-*Stat3*siRNA on tumors

The effects of CpG-siRNA on transferred CD8^{+} T cells in the tumor draining lymph nodes shown in Figure 3 were assessed in mice during a short treatment interval. We next tested

whether the improved effector functions of transferred $CD8^+$ T cells induced by CpG-*Stat3*siRNA could lead to more potent antitumor activity in $B16^{OVA}$ tumor-bearing mice with extended treatment. Again, $CD8^{OT\text{-}I}$ T cells isolated from tumor draining lymph nodes showed significantly increased production of IFN-γ upon recalling $CD8^{OT\text{-}I}$ stimulation with OVA-peptide, thus indicating improved effector CTL conversion upon treatment with CpG-*Stat3*siRNA compared to CpG-*luciferase*-siRNA (Fig. 4*A*). Moreover, targeting *Stat3* in the myeloid compartment using CpG-siRNA resulted in increased activation of $CD8^{OT\text{-}I}$ T cells within tumors after 2 weeks of treatment, as shown by flow cytometric analysis (Fig. 4*B*). Notably, while combining CpG-*luciferase*-siRNA and T cell transfer did not prevent tumor outgrowth, treatment with CpG-*Stat3*siRNA greatly enhanced the antitumor efficacy of adoptively transferred $CD8^{OT\text{-}I}$ T cells (Supplementary Fig. 2*A*). Correlating with significantly elevated IFN-γ production, VCAM-1 expression increased on tumor-associated $CD31^+$ endothelial cells upon treatment with CpG-*Stat3*siRNA and adoptive T cell transfer (Supplementary Fig. 2*B*).

Furthermore, the immunosuppressive $CD4^+CD25^+Foxp3^+$ T_{reg} cell population decreased dramatically upon treatment with CpG-*Stat3*siRNA and $CD8^{OT\text{-}I}$ T cell transfer compared to combination of CpG-*luciferase*-siRNA and T cell transfer (Fig. 4*C*, *top panels*), which was validated by 2-photon microscopy using Foxp3-GFP mice (Fig. 4*C*, *lower panels*). Although T cell transfer alone resulted in a diminished T_{reg} cell population compared to untreated control, treatment with CpG-*luciferase*-siRNA alone did not affect the T_{reg} population. Combining $CD8^{OT\text{-}I}$ T cell adoptive transfer with CpG-*luciferase*-siRNA treatment increased the T_{reg} population, indicating a rather undesired but known effect of TLR9 agonist (34,35). Related to this observation, it has been reported that CpG can activate Stat3, constraining antitumor immune responses (24,36,37). Finally, we analyzed the induction of direct tumor cell apoptosis by multi-photon microscopy *in vivo*. CpG-*Stat3*siRNA treatment for 2 weeks in mice receiving $CD8^{OT\text{-}I}$ T cell transfer resulted in markedly increased induction of tumor cell apoptosis while combination of T cell transfer and CpG-*luciferase*-siRNA did not affect tumor cell viability *in vivo* (Fig. 4*D*). In addition, tumor vasculature collapsed in mice treated with CpG-*Stat3*siRNA and $CD8^{OT\text{-}I}$ T cell adoptive transfer, but was still intact in CpG-*luciferase*-siRNA treated mice. Hence, targeting *Stat3* with CpG-siRNA in the myeloid compartment improves the antitumor efficacy of T cell therapy, achieving robust $CD8^+$ T cell activation and conversion into a CTL phenotype *in vivo*, mounting desired antitumor activity.

CpG-*Stat3*siRNA administration augments anti-tumoral efficacy of transferred $CD8^+$ T cells in a lymphodepletion model

Since T cell therapy is often performed in lymphodepleted setting, and to separate the effects of Stat3 inhibition in myeloid cells on host vs. transferred T cells, we addressed the anti-tumor efficacy of CpG-*Stat3*siRNA administration combined with T cell transfer in B16 melanoma tumor bearing $Rag1^{-/-}$ mice. The tumors in $Rag1^{-/-}$ mice repopulated with $CD8^+$ T cells underwent growth regression upon CpG-*Stat3*siRNA treatment, while the tumors in the $Rag1^{-/-}$ mice treated with CpG-*luciferase*-siRNA/$CD8^+$ T cells continued to grow (Fig. 5*A*). In contrast, the CpG-*Stat3*siRNA administration alone did not completely inhibit growth of B16 tumors in wild-type mice indicating that host CD8 T cell population is insufficient for a desired anti-tumor response. Furthermore, adoptively transferred CD8 cells in B16 tumor bearing $Rag1^{-/-}$ mice treated with CpG-*Stat3*siRNA displayed increased expression of both granzyme B and IFN-γ upon re-stimulation by natural B16 melanoma antigens *ex vivo* (Fig. 5*B*). Moreover, a significant B16 tumor regression was observed in $Rag1^{-/-}$ mice receiving CD8 T cells and CpG-*Stat3*siRNA, but not in the same mice receiving control CpG-scrambled-RNA or CD8 T cell therapy alone (Fig. 5*C*). The expression of both granzyme B as well as IFN-γ protein by adoptively transferred CD8 T

cells isolated from tumor draining lymph nodes was considerably increased upon CpG-*Stat3*siRNA administration (Fig. 5*D*).

Discussion

Current T cell therapies, most notably adoptive T cell therapies, require *ex vivo* activation, expansion and/or genetic engineering, to generate a desired CTL phenotype. This prolonged and extensive *ex vivo* requirement not only limits T cell therapy application but also delays patient treatment. Furthermore, the tumor microenvironment poses a serious threat to dampen the effector functions of transferred T cells and constrains their persistence in the hosts (9). It is therefore highly desirable to identify approaches that can reduce or minimize the requirement for *ex vivo* manipulation of T cells prior to transfer and, perhaps even more importantly, to circumvent the immunosuppressive tumor milieu that interferes the effector functions of transferred T cells. We show here, using genetic approaches, that inhibiting Stat3 in the myeloid compartment and B cells can facilitate the achievement of this goal.

We have recently developed an siRNA delivery technology involving CpG-siRNA conjugate that facilitates siRNA uptake and gene silencing in myeloid cells and B cells. Although CpG driven immune activation is thought to be mainly mediated by TLR9 expressing DCs and TLR9 expression is more restricted among human DCs compared to mouse, macrophages and B cells can also serve as antigen-presenting cells (38). In addition, both macrophages and B cells are important components of the tumor microenvironment, producing immunosuppressive and angiogenic/metastatic factors (39–42). At the same time, human B cells and plasmacytoid DCs, which play an important role in generating anti-tumor immune responses, do express TLR9 (38,43). These findings support further development of human CpG-*Stat3*siRNA for the potential use in the setting of adoptive T cell therapy.

Although our current study only tested CpG-*Stat3*siRNA to improve the effector functions of adoptively transferred T cells *in vivo*, the genetic studies presented here suggest the possible use of other Stat3 inhibitors. Currently, no direct Stat3 inhibitors are in clinical trials. This is largely due to the fact that Stat3 is a transcription factor which, unlike tyrosine kinases, lacks enzymatic activity and is therefore difficult to drug. The use of siRNA based therapy, therefore, is an attractive alternative approach to block Stat3 signaling. On the other hand, Stat3 is a point of convergence for many tyrosine kinase signaling pathways, and certain tyrosine kinase inhibitors in the clinic have been shown to inhibit Stat3 in tumor, including myeloid cells (44). In particular, sunitinib, which has been shown to reduce immunosuppressive T_{regs} and myeloid derived suppressor cells in both patients and mouse tumor models, can inhibit Stat3 activity (45–48). In addition to sunitinib, it is possible to test other tyrosine kinase inhibitors for their potential in enhancing antitumor immune responses. Our findings thus suggest the use of Stat3 inhibitors, including CpG-*Stat3*siRNA, to improve the efficacies as well as broaden the applicability of adoptive T cell therapy.

Supplementary Material

Refer to Web version on PubMed Central for supplementary material.

Abbreviations

C/L	CpG-*luciferase*-siRNA
C/S	CpG-*Stat3*-siRNA
Stat3	Signal transducer and activator of transcription 3

IVMPM adoptive T cell therapy; intravital multiphoton imaging

Acknowledgments

We thank Dr. Piotr Swiderski (City of Hope, Duarte, CA) for CpG and CpGsiRNA synthesis, Dr. Chih-Pin Liu (City of Hope, Duarte, CA) for generously providing us CD11c(YFP)$^{+}$ mice, Dr. Yong Liu for superb assistance, the members of Flow cytometry core, the Light Microscopy Core and Animal Facility at City of Hope for their contributions. This study was supported by the National Institutes of Health (grants R01CA122976 and R01CA146092).

References

1. Gattinoni L, Powell DJ Jr, Rosenberg SA, Restifo NP. Adoptive immunotherapy for cancer: building on success. Nat Rev Immunol. 2006; 6(5):383–393. [PubMed: 16622476]
2. Rosenberg SA, Yang JC, Restifo NP. Cancer immunotherapy: moving beyond current vaccines. Nat Med. 2004; 10(9):909–915. [PubMed: 15340416]
3. Waldmann TA. Effective cancer therapy through immunomodulation. Annu Rev Med. 2006; 57:65–81. [PubMed: 16409137]
4. Rosenberg SA. Progress in human tumour immunology and immunotherapy. Nature. 2001; 411(6835):380–384. [PubMed: 11357146]
5. Leen AM, Rooney CM, Foster AE. Improving T cell therapy for cancer. Annu Rev Immunol. 2007; 25:243–265. [PubMed: 17129181]
6. Zhang B, Bowerman NA, Salama JK, et al. Induced sensitization of tumor stroma leads to eradication of established cancer by T cells. J Exp Med. 2007; 204(1):49–55. [PubMed: 17210731]
7. Brown CE, Vishwanath RP, Aguilar B, et al. Tumor-derived chemokine MCP-1/CCL2 is sufficient for mediating tumor tropism of adoptively transferred T cells. J Immunol. 2007; 179(5):3332–3341. [PubMed: 17709550]
8. June CH. Adoptive T cell therapy for cancer in the clinic. J Clin Invest. 2007; 117(6):1466–1476. [PubMed: 17549249]
9. June CH. Principles of adoptive T cell cancer therapy. J Clin Invest. 2007; 117(5):1204–1212. [PubMed: 17476350]
10. Rosenberg SA, Dudley ME. Adoptive cell therapy for the treatment of patients with metastatic melanoma. Curr Opin Immunol. 2009; 21(2):233–240. [PubMed: 19304471]
11. Yee C, Thompson JA, Byrd D, et al. Adoptive T cell therapy using antigen-specific CD8+ T cell clones for the treatment of patients with metastatic melanoma: in vivo persistence, migration, and antitumor effect of transferred T cells. Proc Natl Acad Sci USA. 2002; 99(25):16168–16173. [PubMed: 12427970]
12. Berger C, Jensen MC, Lansdorp PM, Gough M, Elliott C, Riddell SR. Adoptive transfer of effector CD8+ T cells derived from central memory cells establishes persistent T cell memory in primates. J Clin Invest. 2008; 118(1):294–305. [PubMed: 18060041]
13. Boon T, Coulie PG, Van den Eynde BJ, van der Bruggen P. Human T cell responses against melanoma. Annu Rev Immunol. 2006; 24:175–208. [PubMed: 16551247]
14. Uyttenhove C, Pilotte L, Theate I, et al. Evidence for a tumoral immune resistance mechanism based on tryptophan degradation by indoleamine 2,3-dioxygenase. Nat Med. 2003; 9(10):1269–1274. [PubMed: 14502282]
15. Gajewski TF, Meng Y, Blank C, et al. Immune resistance orchestrated by the tumor microenvironment. Immunol Rev. 2006; 213:131–145. [PubMed: 16972901]
16. Yu H, Pardoll D, Jove R. STATs in cancer inflammation and immunity: a leading role for STAT3. Nat Rev. 2009; 9(11):798–809.
17. Kortylewski M, Kujawski M, Wang T, et al. Inhibiting Stat3 signaling in the hematopoietic system elicits multicomponent antitumor immunity. Nat Med. 2005; 11(12):1314–1321. [PubMed: 16288283]

18. Ho HH, Ivashkiv LB. Role of STAT3 in type I interferon responses. Negative regulation of STAT1-dependent inflammatory gene activation. J Biol Chem. 2006; 281(20):14111–14118. [PubMed: 16571725]
19. Kortylewski M, Yu H. Role of Stat3 in suppressing anti-tumor immunity. Curr Opin Immunol. 2008; 20(2):228–233. [PubMed: 18479894]
20. Yu H, Kortylewski M, Pardoll D. Crosstalk between cancer and immune cells: role of STAT3 in the tumour microenvironment. Nat Rev Immunol. 2007; 7(1):41–51. [PubMed: 17186030]
21. Conroy H, Marshall NA, Mills KH. TLR ligand suppression or enhancement of Treg cells? A double-edged sword in immunity to tumours. Oncogene. 2008; 27(2):168–180. [PubMed: 18176598]
22. Samarasinghe R, Tailor P, Tamura T, Kaisho T, Akira S, Ozato K. Induction of an anti-inflammatory cytokine, IL-10, in dendritic cells after toll-like receptor signaling. J Interferon Cytokine Res. 2006; 26(12):893–900. [PubMed: 17238832]
23. Akira S, Takeda K. Toll-like receptor signalling. Nat Rev Immunol. 2004; 4(7):499–511. [PubMed: 15229469]
24. Kortylewski M, Kujawski M, Herrmann A, et al. Toll-like receptor 9 activation of signal transducer and activator of transcription 3 constrains its agonist-based immunotherapy. Cancer Res. 2009; 69(6):2497–2505. [PubMed: 19258507]
25. Kortylewski M, Swiderski P, Herrmann A, et al. In vivo delivery of siRNA to immune cells by conjugation to a TLR9 agonist enhances antitumor immune responses. Nat Biotech. 2009; 27(10): 925–932.
26. Lee CK, Raz R, Gimeno R, et al. STAT3 is a negative regulator of granulopoiesis but is not required for G-CSF-dependent differentiation. Immunity. 2002; 17(1):63–72. [PubMed: 12150892]
27. Cahalan MD, Parker I. Choreography of cell motility and interaction dynamics imaged by two-photon microscopy in lymphoid organs. Annu Rev Immunol. 2008; 26:585–626. [PubMed: 18173372]
28. Henrickson SE, von Andrian UH. Single-cell dynamics of T-cell priming. Curr Opin Immunol. 2007; 19(3):249–258. [PubMed: 17433876]
29. Mempel TR, Henrickson SE, Von Andrian UH. T-cell priming by dendritic cells in lymph nodes occurs in three distinct phases. Nature. 2004; 427(6970):154–159. [PubMed: 14712275]
30. Schwartz RH. T cell anergy. Annu Rev Immunol. 2003; 21:305–334. [PubMed: 12471050]
31. Rose DM, Alon R, Ginsberg MH. Integrin modulation and signaling in leukocyte adhesion and migration. Immunol Rev. 2007; 218:126–134. [PubMed: 17624949]
32. Lugade AA, Sorensen EW, Gerber SA, Moran JP, Frelinger JG, Lord EM. Radiation-induced IFN-gamma production within the tumor microenvironment influences antitumor immunity. J Immunol. 2008; 180(5):3132–3139. [PubMed: 18292536]
33. Denucci CC, Mitchell JS, Shimizu Y. Integrin function in T-cell homing to lymphoid and nonlymphoid sites: getting there and staying there. Crit Rev Immunol. 2009; 29(2):87–109. [PubMed: 19496742]
34. Krieg AM. Development of TLR9 agonists for cancer therapy. J Clin Invest. 2007; 117(5):1184–1194. [PubMed: 17476348]
35. Moseman EA, Liang X, Dawson AJ, et al. Human plasmacytoid dendritic cells activated by CpG oligodeoxynucleotides induce the generation of CD4+CD25+ regulatory T cells. J Immunol. 2004; 173(7):4433–4442. [PubMed: 15383574]
36. Wingender G, Garbi N, Schumak B, et al. Systemic application of CpG-rich DNA suppresses adaptive T cell immunity via induction of IDO. Eur J Immunol. 2006; 36(1):12–20. [PubMed: 16323249]
37. Mellor AL, Baban B, Chandler PR, Manlapat A, Kahler DJ, Munn DH. Cutting edge: CpG oligonucleotides induce splenic CD19+ dendritic cells to acquire potent indoleamine 2,3-dioxygenase-dependent T cell regulatory functions via IFN Type 1 signaling. J Immunol. 2005; 175(9):5601–5605. [PubMed: 16237046]
38. Krieg AM. Therapeutic potential of Toll-like receptor 9 activation. Nat Rev Drug Discov. 2006; 5(6):471–484. [PubMed: 16763660]

39. Kortylewski M, Xin H, Kujawski M, et al. Regulation of the IL-23 and IL-12 balance by Stat3 signaling in the tumor microenvironment. Cancer Cell. 2009; 15(2):114–123. [PubMed: 19185846]
40. Takeda K, Clausen BE, Kaisho T, et al. Enhanced Th1 activity and development of chronic enterocolitis in mice devoid of Stat3 in macrophages and neutrophils. Immunity. 1999; 10(1):39–49. [PubMed: 10023769]
41. Kujawski M, Kortylewski M, Lee H, Herrmann A, Kay H, Yu H. Stat3 mediates myeloid cell-dependent tumor angiogenesis in mice. J Clin Invest. 2008; 118(10):3367–3377. [PubMed: 18776941]
42. Tan TT, Coussens LM. Humoral immunity, inflammation and cancer. Curr Opin Immunol. 2007; 19(2):209–216. [PubMed: 17276050]
43. Iwasaki A, Medzhitov R. Toll-like receptor control of the adaptive immune responses. Nat Immunol. 2004; 5(10):987–995. [PubMed: 15454922]
44. Kim LC, Song L, Haura EB. Src kinases as therapeutic targets for cancer. Nat Rev Clin Oncol. 2009; 6(10):587–595. [PubMed: 19787002]
45. Xin H, Zhang C, Herrmann A, Du Y, Figlin R, Yu H. Sunitinib inhibition of Stat3 induces renal cell carcinoma tumor cell apoptosis and reduces immunosuppressive cells. Cancer Res. 2009; 69(6):2506–2513. [PubMed: 19244102]
46. Yang F, Jove V, Xin H, Hedvat M, Van Meter TE, Yu H. Sunitinib induces apoptosis and growth arrest of medulloblastoma tumor cells by inhibiting STAT3 and AKT signaling pathways. Mol Cancer Res. 8(1):35–45. [PubMed: 20053726]
47. Ozao-Choy J, Ma G, Kao J, et al. The novel role of tyrosine kinase inhibitor in the reversal of immune suppression and modulation of tumor microenvironment for immune-based cancer therapies. Cancer Res. 2009; 69(6):2514–2522. [PubMed: 19276342]
48. Ko JS, Zea AH, Rini BI, et al. Sunitinib mediates reversal of myeloid-derived suppressor cell accumulation in renal cell carcinoma patients. Clin Cancer Res. 2009; 15(6):2148–2157. [PubMed: 19276286]

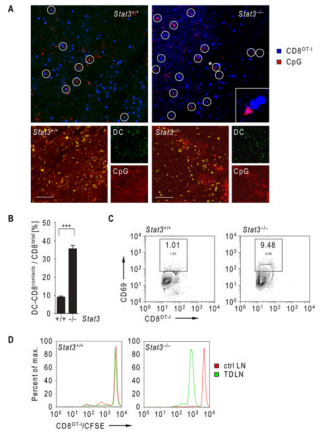

Figure 1.

Genetic ablation of *Stat3* enhances DC engagement and expansion of adoptively transferred CD8^{OT-I} cells. *A*, Top two panels - engagement of adoptively transferred CD8^{OT-I} T cell by DCs (*white circles*) in the TDLN of mice with *Stat3*$^{+/+}$ and *Stat3*$^{-/-}$ myeloid compartment 24 h after T cell transfer. CD8^{+} cells were fluorescently labeled using CMAC (*blue*) and adoptively transferred after peritumoral injection of fluorescent CpG-Alexa555 (*red*). Cell to cell contacts were monitored by IVMPM *in vivo*. The asterisk indicates contact event shown enlarged in the lower right corner (top right panel). Bottom panels - confocal micrographs of TDLNs of mice with *Stat3*$^{+/+}$ and *Stat3*$^{-/-}$ myeloid cells showing CpG (*red*) uptake by DCs (*green*). Scale bar = 100 μm. *B*, DC/CD8^{OT-I} contacts in TDLNs were quantified in three independent experiments as described above. Shown are the means ± S.D.; n = 4. Statistically significant differences between both groups were analyzed by student's t-test and labeled as ***, $P < 0.001$. *C*, Activation of adoptively transferred CD8^{OT-I} in TDLNs of mice with *Stat3*$^{+/+}$ and *Stat3*$^{-/-}$ myeloid compartment 24 h after T cell transfer. The expression of CD69 on fluorescently labeled CD8^{OT-I} cells was analyzed using FACS. Shown are representative results from two independent experiments using TDLNs pooled from four mice per group. *D*, The proliferation of CD8^{OT-I} cells adoptively transferred into mice with *Stat3*$^{+/+}$ or *Stat3*$^{-/-}$ myeloid compartment. The proliferation of CFSE-labeled CD8^{OT-I} cells was assessed by FACS analysis in TDLNs (*green*) or contralateral LNs (*red*) 24 h after adoptive transfer. Shown are representative results from one of three independent experiments using pooled TDLNs (n = 3).

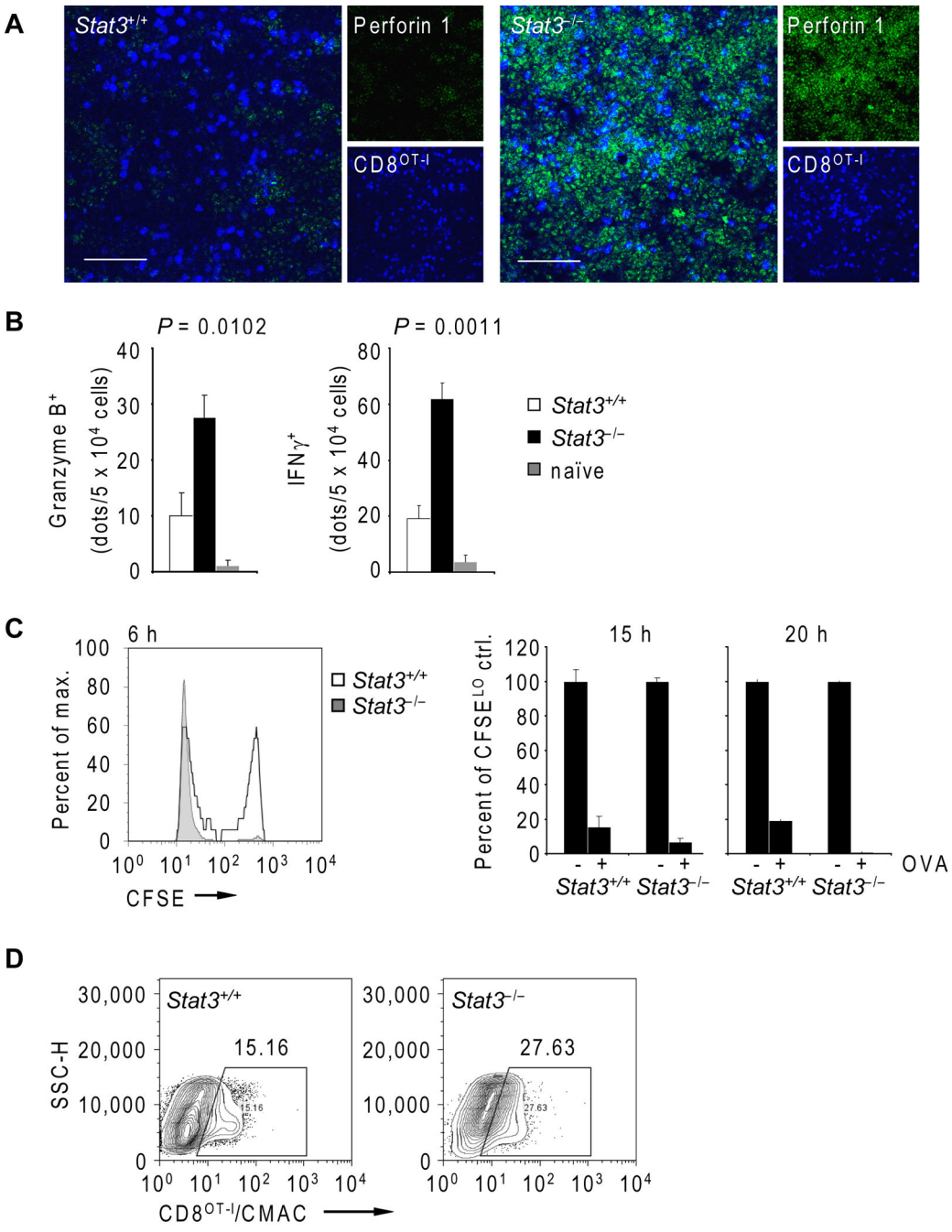

Figure 2.

Stat3 ablation in the myeloid compartment improves antigen-specific CTL maturation and tumor infiltration following adoptive transfer of $CD8^{OT\text{-}I}$ cells. *A*, Confocal micrographs of TDLNs of mice with $Stat3^{+/+}$ and $Stat3^{-/-}$ myeloid cells 24 h after adoptive transfer show $CD8^{OT\text{-}I}$ cells (blue, fluorescently labeled using CMAC) and perforin 1 expression (*green*, immunofluorescent staining). Shown are representative images from two independent experiments; scale bar 50 μm. *B*, Lack of *Stat3* in myeloid cells results in higher production of granzyme B and IFN-γ by adoptively transferred OVA-specific $CD8^{OT\text{-}I}$ T cells. ELISPOT assay was performed 24 h after adoptive T cell transfer into mice with $Stat3^{+/+}$ or $Stat3^{-/-}$ myeloid compartments. Naïve lymphocytes were included as a control. Shown are

means ± S.E.M. from two independent experiments using four mice/group as analyzed by one-way ANOVA. *C, In vivo* CTL killing assay using a pool of $OVA^{SIINFEKL}$-pulsed $CFSE^{HI}$ and off-target $CFSE^{LO}$ splenocytes was performed 24 h after adoptive transfer of $CD8^{OT\text{-}I}$ T cells to $Stat3^{+/+}$ (*white*) and $Stat3^{-/-}$ (*grey*) tumor-bearing mice. The percentages of CFSE-positive $CD8^{OT\text{-}I}$ cells in TDLNs were assessed by flow cytometry at times as indicated. Shown are means ± S.E.M. for two independent experiments performed in triplicates per each time point (*right panel*). *D*, Tumor infiltration by fluorescently labeled $CD8^{OT\text{-}I}$ T cells 24 h after adoptive transfer into mice with $Stat3^{+/+}$ or $Stat3^{-/-}$ myeloid compartment was analyzed by flow cytometry. Shown are representative results from one of two experiments using cells pooled from at least three tumors/group.

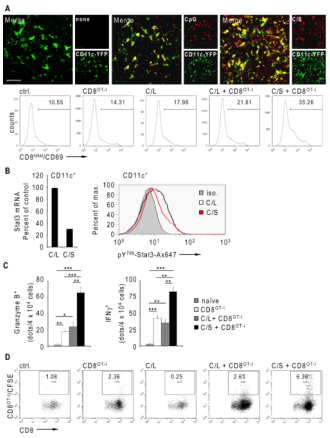

Figure 3.

CTL maturation and tumor infiltration of adoptively transferred $CD8^+$ T cells are enhanced by *Stat3* silencing in myeloid cells *in vivo*. *A*, Top row - *in vivo* uptake of fluorescently labeled CpG (*red*) or CpG-*Stat3*siRNA (*C/S, red*) by $CD11c^+$ (*green*) DCs. Naïve CD11c-YFP mice were injected *s.c.* using equimolar amounts of CpG (*middle panel*) or CpG-*Stat3*siRNA (C/S, *right panel*) or left untreated (*left panel*). The oligonucleotide uptake and DC trafficking into lymph nodes was visualized 2 h later by IVMPM; red and green channels are shown separately next to the overlay; scale bar = 50 μm. Bottom row – B16-OVA tumor-bearing mice received adoptive transfer of $CD8^{OT\text{-}I}$ T cells in combination with three peritumoral injections of either CpG-*Stat3*siRNA (C/S) or CpG-*luciferase*-siRNA (C/L). Mice without treatment or treated only with CpG-*luciferase*-siRNA or by adoptive T cell transfer alone were used as controls. $CD8^+$ T cell activation determined by the level of CD69 expression was measured by FACS 24 h after the last injection. Data shown are representative of two independent experiments from pooled TDLNs (n=4). *B*, *Stat3* mRNA expression and the level of activated Stat3 protein in $CD11c^+$ cells isolated from TDLNs (*left panel*) or TMs (*right panel*), respectively. Mice were treated thrice with indicated siRNAs and evaluated by quantitative real-time PCR and flow cytometry. *C*, Granzyme B and IFN-γ production from TDLN lymphocytes of tumor bearing treated as indicated was assessed by ELISPOT assay. Shown are means ± S.E.M. (n=4). Statistically significant differences between analyzed groups were determined by one-way ANOVA; ***, $P < 0.001$; **, $P < 0.01$; *, $P < 0.05$. Data shown are representative of two independent experiments using pooled TDLN cells (n=3). *D*, Tumor infiltration by adoptively transferred $CD8^{OT\text{-}I}$ T cells was analyzed by flow cytometry. Mice were treated thrice as indicated above. Data shown are representative of two independent experiments using cells pooled from four tumors/group.

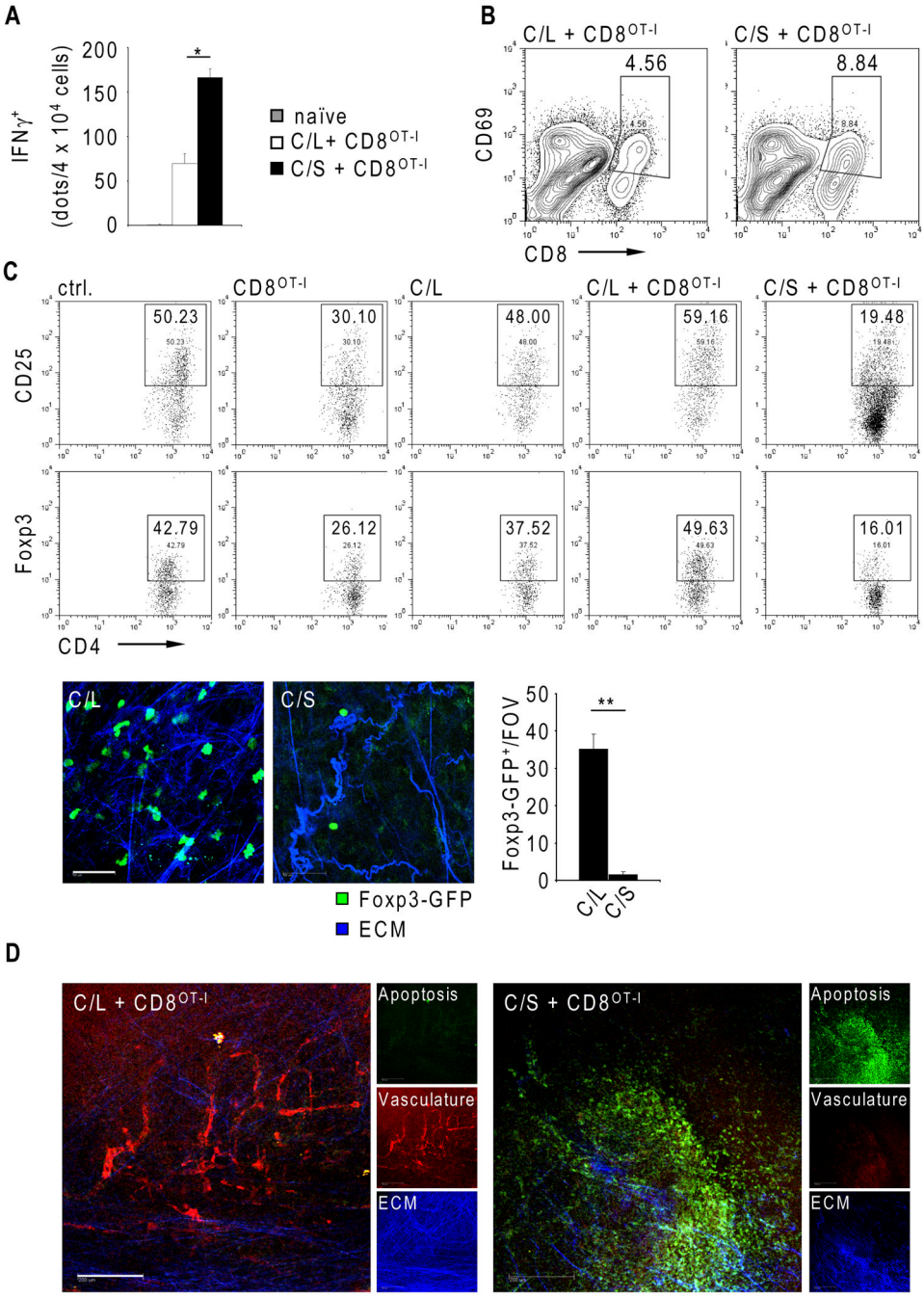

Figure 4.

CpG-*Stat3*siRNA mediated knockdown improves $CD8^+$ T cell therapy. Tumor bearing mice were treated seven times with CpG-*luciferase*-siRNA or CpG-*Stat3*siRNA combined with $CD8^{OT-I}$ adoptive transfer. *A*, IFN-γ production by CD8 T cells isolated from TDLN after prolonged *Stat3* silencing was assessed by ELISPOT. Shown are the means ± SD; n = 4. Statistically significant differences between analyzed groups were labeled as *, $P<0.05$ by student's *t*-test. *B*, The activation of tumor-infiltrating $CD8^+$ cells was assessed by CD69 expression using flow cytometry. *C*, Top – the percentages of tumor-infiltrating T_{regs} from mice receiving indicated treatments were quantified by flow cytometry. Shown are representative results from two independent experiments on tumors pooled from four mice/

group. Bottom – *Stat3* silencing reduces number of tumor-infiltrating Tregs in transgenic Foxp3-GFP mice. The GFP-positive T_{regs} were visualized by IVMPM in B16 tumors following treatment using siRNA conjugates as indicated (left panels). T_{reg} numbers were quantified using three independent field of views (FOV) (*right panel*); *P* value by student's *t*-test was labeled as **, $P < 0.01$; scale bar 50 μm. *D*, Tumor vascularization and apoptosis was analyzed by IVMPM after adoptive transfer of $CD8^{OT\text{-}I}$ cells and prolonged treatment with siRNA conjugates, as indicated. Early apoptotic events (*green*), neovasculature (*red*), and ECM (*blue*) are shown separately next the overlay; scale bar = 200 μm. Shown are results from two independent experiments using two mice/group.

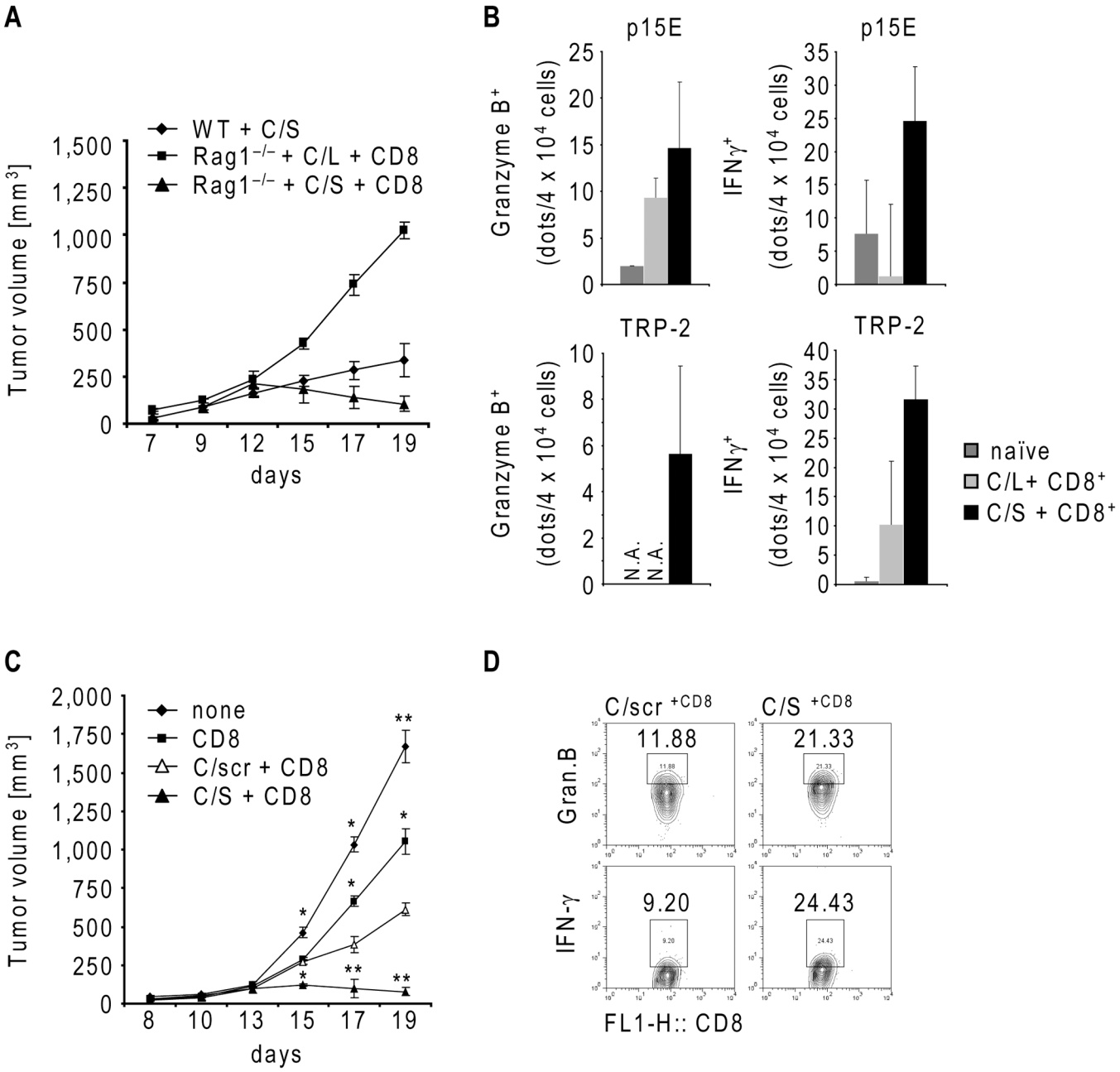

Figure 5.

CpG-*Stat3*siRNA in combination with adoptive CD8 T cell transfer augments antigen-specific immune responses resulting in tumor regression in lymphopenic mouse model. *A*, B16 melanoma tumor growth kinetics in C57BL/6 wild-type mice or Rag1$^{-/-}$ mice treated as indicated (n=4); shown are means ± S.D. *B*, B16 tumor antigen-specific granzyme B and IFN-γ production by TDLN lymphocytes was assessed by ELISPOT upon p15E (top) or TRP-2 (bottom) stimulation; shown are mean numbers of spots ± S.D. (n=3). *C*, B16 tumor growth in Rag1$^{-/-}$ mice with indicated treatments. Shown are means ± S.D. (n=4); statistically significant differences were indicated as: **, $P < 0.01$; *, $P < 0.05$. *D*, *Stat3* targeting in the myeloid compartment enhances granzyme B and IFN-γ expression by

adoptively transferred CD8 cells. TDLN cells from mice (n=4) after prolonged CpG-siRNA treatments, as indicated, were analyzed by intracellular staining and flow cytometry.